

## **A STUDY OF THE EFFECT OF ELEMENT TYPES ON FLOW AND TURBULENCE CHARACTERISTICS AROUND AN ISOLATED HIGH-RISE BUILDING**

**M Zahid IQBAL<sup>1\*</sup> and ALS CHAN<sup>2</sup>**

<sup>1</sup> Department of Architecture and Civil Engineering, College of Science and Engineering,  
City University of Hong Kong, Hong Kong

<sup>2</sup> Division of Building Science and Technology, College of Science and Engineering,  
City University of Hong Kong, Hong Kong

\*Corresponding author, E-mail address: muqureshi3-c@my.cityu.edu.hk

### **ABSTRACT**

Grid generation is a crucial and time-intensive numerical simulation process in which element type and mesh density play a major role. The accuracy and high computational cost of numerical simulations remain an academic and industrial challenge. This study quantitatively assessed the effect of an element type on the flow and turbulence characteristics around an isolated high-rise building through a Reynolds-averaged Navier-Stokes turbulence model. Hexahedral and tetrahedral elements are commonly used in computational fluid dynamics (CFD) simulations; however, polyhedral elements are rarely used. Hexahedral, polyhedral, and tetrahedral elements were compared, and in each case, coarse, medium, and fine mesh resolutions were investigated. The effects of an element type on the mean flow and turbulent kinetic energy around an isolated high-rise building were discussed. Furthermore, the results were compared against the wind tunnel experimental data reported in relevant literature. The results showed that polyhedral elements performed more favourably than tetrahedral elements. However, the results of hexahedral element were closer to those of the experiment. In addition, a mean absolute error (MAE) was calculated, and the results showed that polyhedral elements required less computational time than tetrahedral elements did. Using polyhedral elements in CFD was found to be more effective than using tetrahedral elements.

**Keywords:** CFD, CWE, mesh generation, element types, bluff body.

### **INTRODUCTION**

With advances in computing power, computational fluid dynamics (CFD) is increasingly becoming a topic of research interest. However, predicting accurate and reliable solutions remains a challenge (Blocken, 2014). Grid generation is the most time intensive and crucial part of CFD analyses. In general, grid generation consumes more than half the time required for the pre-processing and discretization setup of CFD analyses. Computational time also depends on various other factors, such as knowledge and expertise, processing power, and element types. A previous study has shown that element type is an essential factor for obtaining an accurate solution at low computational cost (Hefny & Ooka, 2008). Generally, accuracy and computational cost are determined by the number of cells; that is, more cells indicate high accuracy

and cost, but this is not always true. Accurate and reliable solutions can also be obtained by the appropriately selecting the element types and grid generation methodology, such as structured and unstructured grid formation.

In academia and industry, hexahedral, tetrahedral, and polyhedral elements and their combinations are most commonly used for CFD analyses. Earlier, only hexahedral elements were used because of their flexibility. However, generating hexahedral mesh for complex geometries require time and expertise. By contrast, tetrahedral elements are easy to generate and require less computational cost even for complex geometries; however, the probability of numerical diffusions is high. Furthermore, high densities of small tetra or prismatic elements are required for near-wall treatment. Hexahedral and tetrahedral mesh types have been well studied and have evolved. Furthermore, both mesh types are the standard choice in most CFD packages, because of their robust solution and meshing complex geometries. However, because of numerical instability and convergence problems, the tetrahedral mesh is not an ideal. To solve the aforementioned problems, hybrid techniques and prismatic elements have been used with the tetrahedral elements. Moreover, advanced discretization techniques have been applied to obtain accurate solution; however, these alternatively increase computational cost. Recently, several researchers have used polyhedral elements instead of tetrahedral elements (Peri, 2004; Garimella et al., 2014). They concluded that polyhedral elements can overcome the discrepancies associated with tetrahedral elements using fewer elements and the same level of automatic mesh generation ability. Furthermore, they reported that polyhedral elements are surrounded by more elements than tetrahedral element are, which increase the accuracy of approximate solutions. However, polyhedral elements are computationally more expensive in some cases because of their complex geometry (Berg et al., 2008). In the past, polyhedral elements have received less attention because of the unavailability of polyhedral mesh generation algorithms in CFD codes. However, in the last few years, polyhedral elements have gained more attention.

The aforementioned brief review highlights the gap that exists in studies on grid generation techniques and shows the limited adoption of a polyhedral mesh in CFD analysis. The aforementioned discussions encouraged the authors to further investigate the topic. This study comparatively analyses the three aforementioned elements

in the context of computational wind engineering (CWE). A simple rectangular bluff body, which is a replica of high-rise building, was used in the analysis.

## MODEL DESCRIPTION

### Numerical model

In this study, the CFD code Fluent was used for numerical simulations. Previous studies have shown that the  $k - \varepsilon$  Reynolds-averaged Navier-Stokes (RANS) turbulence models and Reynolds stress models (RSM) provide acceptable solution to outdoor analyses. In this study, the renormalization group (RNG)  $k - \varepsilon$  turbulence model was used for the analysis. The RNG model proposed by (Yakhot, Orszag, Thangam, Gatski, & Speziale, 1992) and several other studies recommended for simulating airflow around the buildings and bluff bodies. The governing equations of RNG  $k - \varepsilon$  turbulence model for turbulent quantities ( $k, \varepsilon$ ) are given as follow:

$k$ -equation

$$\frac{\partial}{\partial t}(\rho k) + \frac{\partial}{\partial x_j}(\rho k u_j) = \frac{\partial}{\partial x_j} \left[ \alpha_k \mu_{eff} \frac{\partial k}{\partial x_j} \right] + G_k + G_b - \rho \varepsilon - Y_M + S_k \quad (1)$$

$\varepsilon$ -equation

$$\frac{\partial}{\partial t}(\rho \varepsilon) + \frac{\partial}{\partial x_j}(\rho \varepsilon u_j) = \frac{\partial}{\partial x_j} \left[ \alpha_\varepsilon \mu_{eff} \frac{\partial \varepsilon}{\partial x_j} \right] + C_{1\varepsilon} \frac{\varepsilon}{k} (G_k + C_{3\varepsilon} G_b) - C_{2\varepsilon} \rho \frac{\varepsilon^2}{k} + S_\varepsilon \quad (2)$$

Where,

$G_k$  = Generation of turbulent Kinetic energy

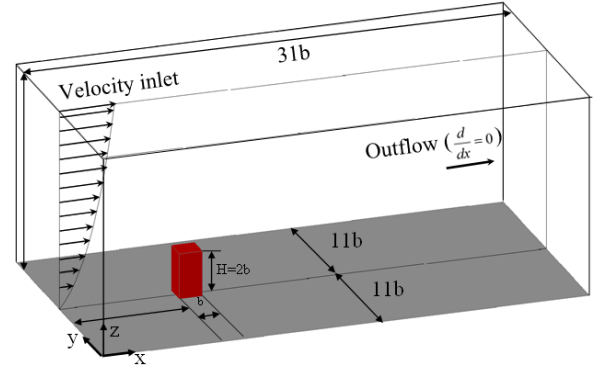
$G_b$  = Generation of turbulent kinetic energy because of Buoyancy

$Y_M$  = Ratio of fluctuation dilatation in compressible turbulence to the overall dissipation rate

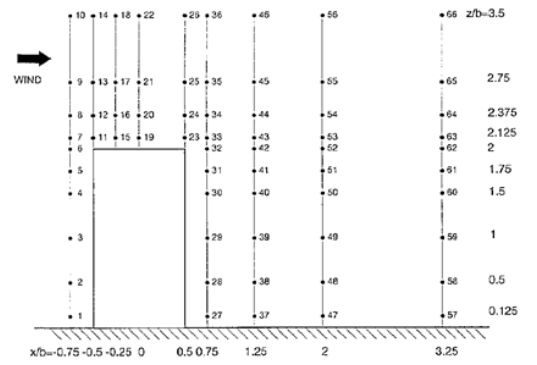
$C_{1\varepsilon}, C_{2\varepsilon}, C_{3\varepsilon}$  are constants;  $\alpha_k$  and  $\alpha_\varepsilon$  are the inverse effective Prandtl numbers for  $k$  and  $\varepsilon$ , respectively; and  $S_k$  &  $S_\varepsilon$  are the source terms.

### Experimental setup

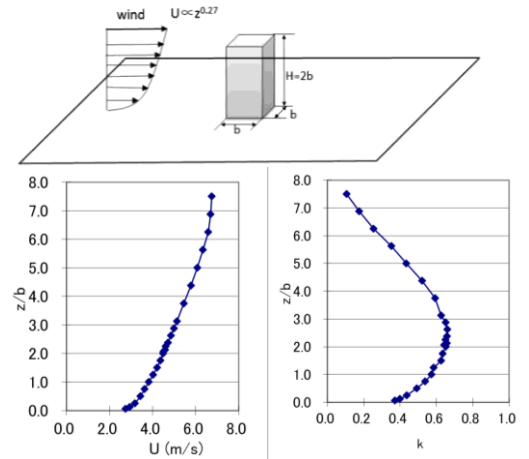
Results of the wind tunnel experiment of flow around a rectangular bluff body, conducted by Mochida et al., (2002) were used for validating the simulation. A rectangular block (Width  $\times$  Depth  $\times$  Height  $0.08\text{m} \times 0.08\text{m} \times 0.16\text{m}$ ) was mounted within the boundary layer wind tunnel, as shown in the Figure 1(a). The detailed of experiment set up and flow field are as reported in Mochida et al., (2002). The locations of the measurement points along the block height are illustrated in Figure 1(b). Several studies have used square block arrangement for evaluating and validating the simulation results, such as (Hefny & Ooka, 2008). On the basis of the previous results, the Reynolds number ( $Re$ ) was set as  $2.4 \times 10^4$ . To adhere the standard domain setup, the boundary condition and approaching wind and TKE profile (Figure 1 (c)) of the Architectural Institute of Japan (AIJ) were used. The Turbulent intensity ( $I_u$ ) profile is defined as  $k = 0.5(I_u U)^2$ . The details of the boundary conditions are as given in (Mochida et al., 2002). The wind and turbulent kinetic energy (TKE) profiles are presented in Figure 1(c).



(a)



(b)



(c)

**Figure 1:** (a) Computational domain setup. (b) Locations of measurement points around the rectangular bluff body. (c) Approaching wind and TKE profiles.

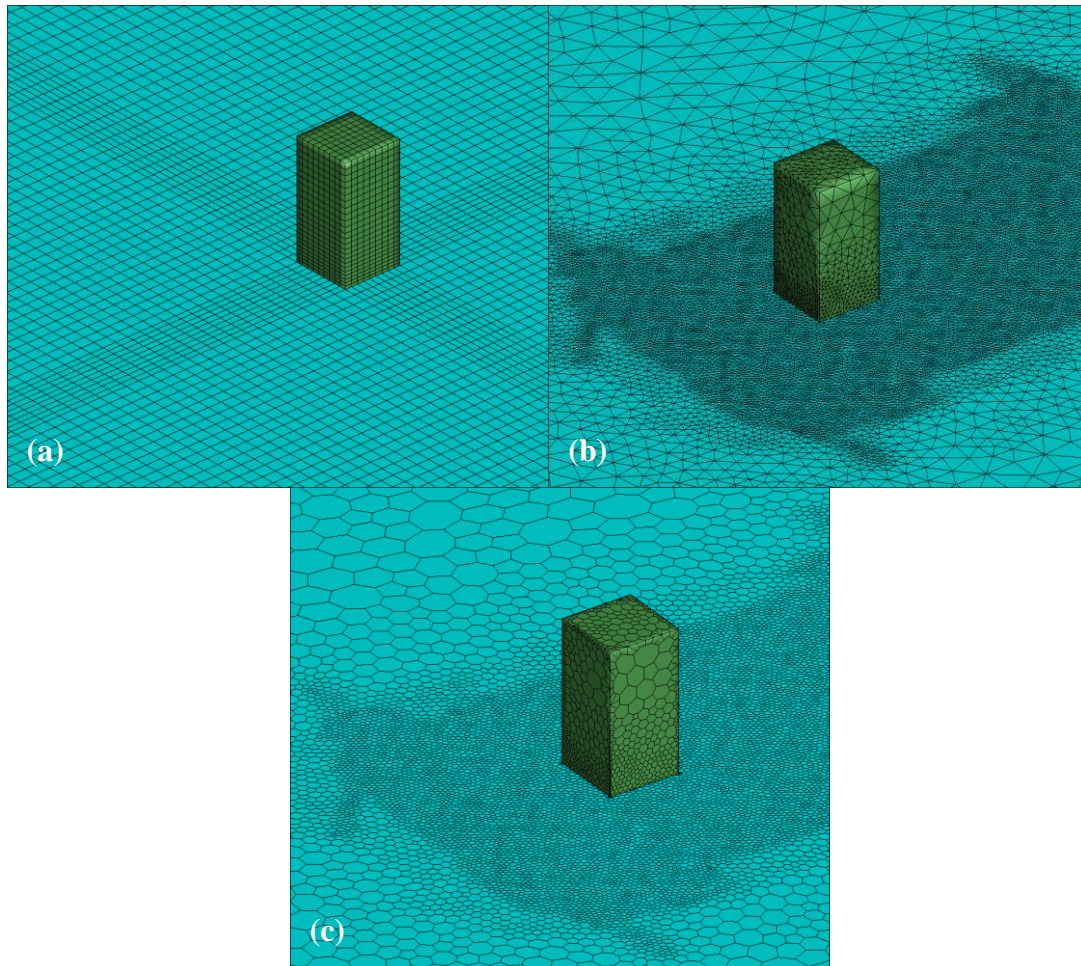


**Figure 2:** Different Grid schemes. (a) Hexahedral. (b) Tetrahedral. (c) Polyhedral.

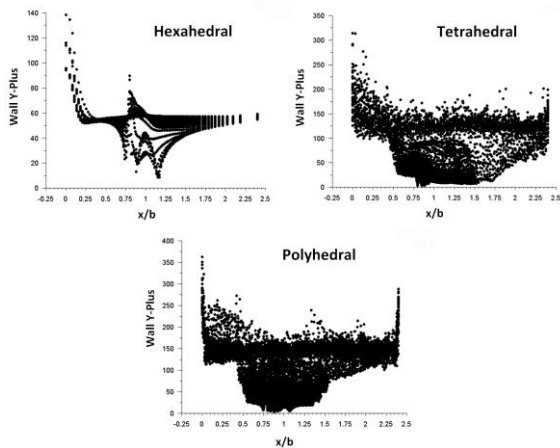


**Figure 3:** Node values of wall y plus.

## RESULTS

In this study, three elements were evaluated using the same discretization schemes and different mesh sizes. Figure 2 shows the three grid schemes. The hexahedral and tetrahedral elements were generated using the ICFM CFD. Tetrahedral elements were converted into polyhedral elements by using the CFD code Fluent. To maintain the near-wall flow, a standard wall function was applied, and y-plus values were maintained between 20 and 200. Figure

3 shows the y-plus values of all the mesh schemes; all node values are between 20 and 200. Only a few points were observed outside the defined range, as shown in Figure 3. Initially, hexahedral and tetrahedral elements were generated using a linear factor of 1.5; however to maintain the y-plus values within the aforementioned limit, high mesh density was applied around the block, as shown in Figures 2 and 3. The convergence level ( $1 \times 10^{-4}$ ) for all mesh sizes and for all parameters was equal. Coarse, medium, and fine mesh sizes were used, as shown in the Table 1 (Grid I–III).

	Hexahedral	Tetrahedral	Polyhedral
<b>Grid-I</b>	$2.3 \times 10^5$	$2.4 \times 10^5$	$5.3 \times 10^4$
<b>Grid-II</b>	$4.2 \times 10^5$	$1.1 \times 10^6$	$1.9 \times 10^5$
<b>Grid-III</b>	$6.2 \times 10^5$	$2.0 \times 10^6$	$3.2 \times 10^5$

**Table 1:** Detailed of mesh resolutions

## Convergence Analysis

Figure 4 demonstrates the convergence behaviour of various parameters. A predefined standard convergence criterion was applied. In the CFD analysis, a satisfactory convergence is based on the mesh size and discretization scheme. Convergence is also dependent on the geometry of the body; the solution of a complex body takes more time to converge than that of simple bodies.

The results demonstrate that the hexahedral solution converged at the maximum number of iterations, and the polyhedral solution converged at the minimum number of iterations. Similar behaviour was observed in medium and fine mesh sizes. All three mesh sizes show smooth and stable convergence behaviour. Polyhedral elements converged at a low number of iterations, and a low number of iterations implies a low computational cost.

In all cases (Grid I–III), the mesh elements in a polyhedral mesh are fewer than in the tetrahedral elements because of the conversion process of tetrahedral elements into polyhedral elements. The iterations in the tetrahedral elements were fewer than those in the hexahedral elements, and higher than those in the polyhedral elements. By adjusting the convergence criteria, the convergence process can be accelerated; however, polyhedral elements provide the solution at standard convergence criteria and low cost.

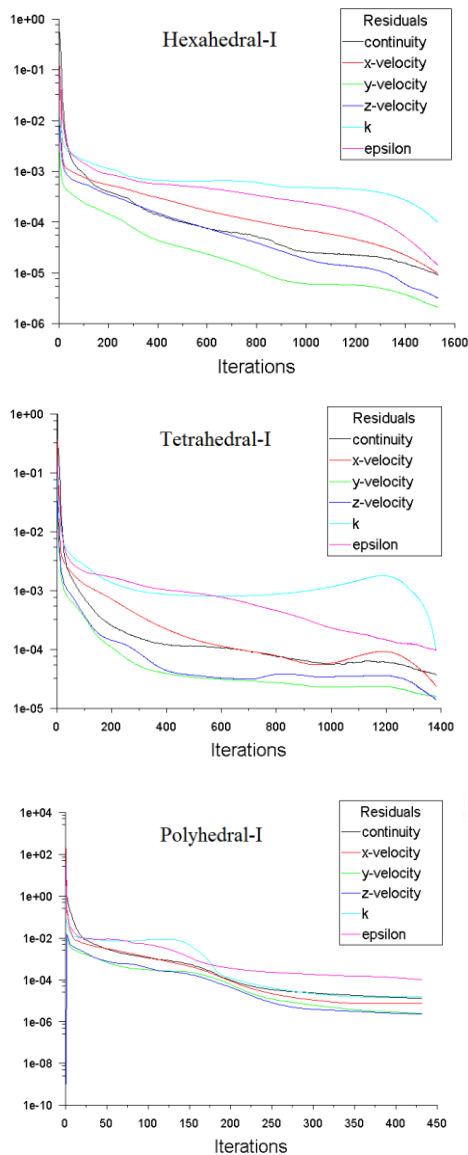


Figure 4: Convergence plot of Grid I.

### Comparison of flow parameters

The wind velocity ( $U$ ) and Turbulent kinetic energy (TKE) parameters at the upstream (one location  $x/b = -0.75$ ) and downstream (two locations  $x/b = 0.75$  &  $x/b = 1.25$ ) sides of the rectangular bluff body were compared. Figure 5 shows the comparison of wind velocity at  $x/b = -0.75, 0.75$  &  $1.25$  and the three grid resolutions. The results demonstrate that the polyhedral solution is closer to the experimental result than the tetrahedral solution is. A small deviation was observed in the polyhedral elements in Grid I, above the height of the bluff body. However in all other cases, polyhedral elements showed more favourable results. In all cases, tetrahedral elements demonstrated nonconformity at the ground level, which is inadequate for near-wall flow analysis.

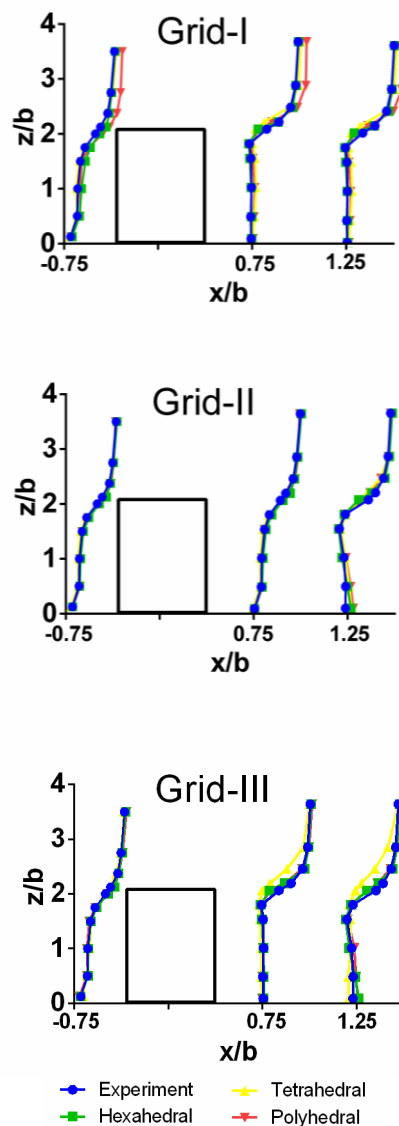
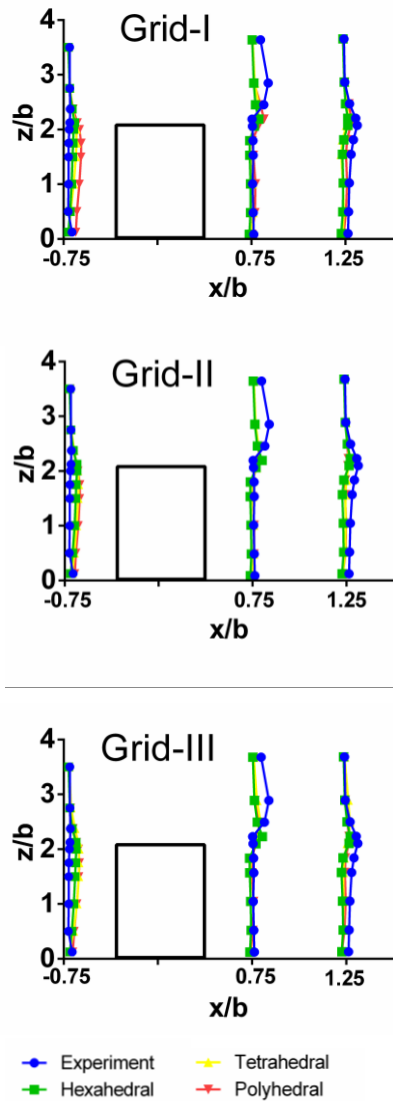


Figure 5: Comparison of wind profile at  $x/b = -0.75, 0.75$  and  $1.25$ .

Similarly, in Grid II, at position  $x/b=0.75$  both elements are good agreement with the experimental results. However, in Grid I and III, tetrahedral elements overestimated and underestimated the wind velocity throughout the block height. In Grid III, all elements showed over- and underestimation because of the wake area that develops at the downstream side of the bluff body. Similar behavior was observed in tetrahedral elements ( $x/b=1.25$ ). Figure 6 depicts TKE at various locations around the body (Figure 1(b)).



**Figure 6:** TKE profile at  $x/b = -0.75, 0.75$  and  $1.25$

At  $x/b = -0.75$ , an overestimation was observed in all cases. Although the deviation was high at low grid resolution, the difference decreased at high grid resolution. At  $x/b = 0.75$ , the underestimation at the ground level is due to the turbulent wake area and stagnation region. At  $x/b = 1.25$ , tetrahedral and

polyhedral elements outperformed the hexahedral elements. In addition, the over and underestimations in tetrahedral elements were because of numerical diffusion, which is common in unstructured meshes. To avoid the diffusion effect, a very fine mesh is required, particularly for tetrahedral elements.

### Mean Absolute Error (MAE) Comparison

The three meshing schemes were further evaluated using the MAE, which was calculated using equation 3.

$$\left( \frac{1}{n} \sum \frac{|Actual - predicted|}{|Actual|} \right) \quad (3)$$

Figure 7 shows a comparison among MAEs of wind profiles at three positions:  $x/b = -0.75, 0.75$ , and  $1.25$ . At  $x/b = -0.75$ , tetrahedral and polyhedral elements show low MAEs in coarse and fine grids, respectively. Similarly, at  $x/b = 0.75$  and  $1.25$ , polyhedral elements shows low MAE compared with the tetrahedral elements in the fine grid.

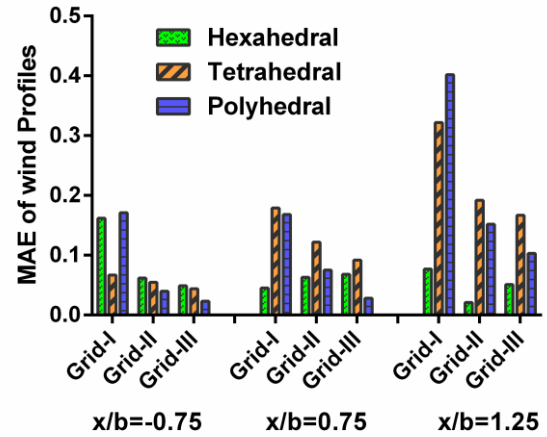


**Figure 7:** Comparison of MAE of wind profiles at  $x/b = -0.75, 0.75$  and  $1.25$ .

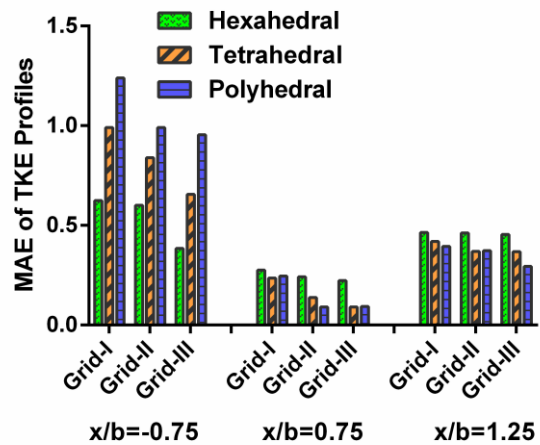


**Figure 8:** Comparison of MAE of TKE at  $x/b = -0.75, 0.75$  and  $1.25$ .

Figure 8 shows the MAE of TKE at three positions. At  $x/b = -0.75$ , tetrahedral elements show less MAE; at  $x/b = 0.75$  and  $1.25$ , polyhedral elements show low MAE compared with both hexahedral and tetrahedral elements. Overall, polyhedral elements outperform tetrahedral elements at a low number of cells.

### Grid Quality

Mesh quality is vital for evaluating the accuracy and stability of the results. The mesh quality in finite volume method (FVM) is measured through various methods. In this study, polyhedral and tetrahedral elements were evaluated using the orthogonal quality index, an essential parameter in almost all CFD code (Canonsburg, 2012). The orthogonal quality of an element is defined as

$$\frac{\vec{A}_i \cdot \vec{f}_i}{A_i \|f_i\|} \quad \text{and} \quad \frac{\vec{A}_i \cdot \vec{C}_i}{A_i \|C_i\|} \quad (4)$$

Where,  $\vec{A}_i$  is the area vector of a face,  $\vec{f}_i$  is the centroid of that face, and  $\vec{C}_i$  is the centroid of that face.

The orthogonal quality varies from 0 to 1; a value close to 0 indicates the worst cells and that close to 1 indicates the optimal orthogonal quality. Figure 9 shows the orthogonal quality of polyhedral and tetrahedral meshes. The results indicate that the polyhedral mesh has a more satisfactory orthogonal quality compared with the tetrahedral mesh.

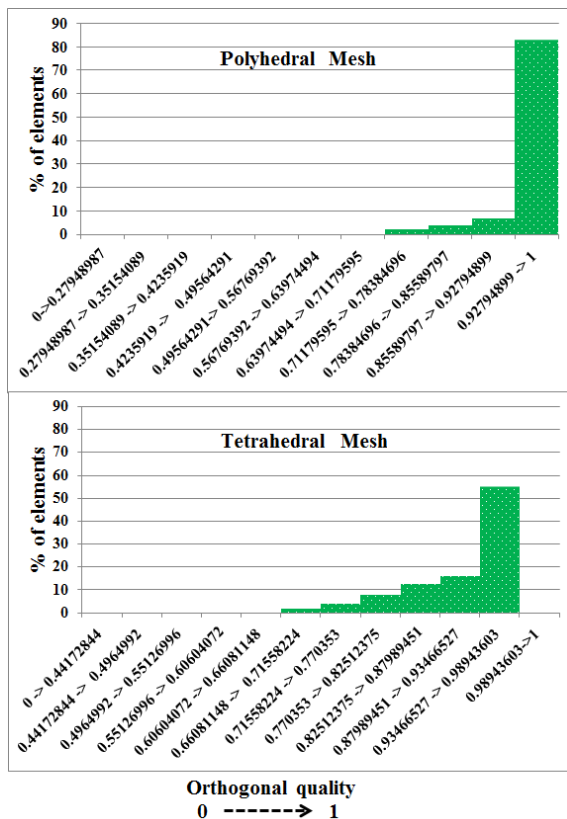


Figure 9: Orthogonal quality plot of polyhedral and tetrahedral meshes.

### CONCLUSION

This study evaluated the performance of polyhedral elements in the context of CWE applications. In addition, tetrahedral and hexahedral elements were compared, and the wind velocity and TKE around the rectangular bluff body were considered. The results were validated using the wind tunnel experiment. A quantitative analysis was performed at three grid resolutions. The results showed that the selection of the element type strongly influence the CFD simulation. A hexahedral element is commonly used for simple geometries because of its high accuracy and stable convergence. However the number of elements and computational cost are higher in hexahedral elements. Therefore, the use of hexahedral elements is limited to simple and symmetrical objects. Tetrahedral and polyhedral elements are used in complicated and nonsymmetrical objects. In this study, polyhedral elements outperformed the other elements in both wind flow and TKE analysis. Convergence analysis demonstrated that in polyhedral elements, convergence was accelerated compared with that in tetrahedral elements. Furthermore, iterations were fewer in polyhedral elements at the same level of convergence criteria. Moreover, the preprocessing time of the polyhedral elements was lesser than that of the tetrahedral elements. Variations in tetrahedral elements were higher because of the diffusion problems associated with tetrahedral elements. To obtain a stable solution, a very fine mesh resolution is required for tetrahedral elements, which increases the computational cost.

The results revealed that the polyhedral element provides an alternative solution at low cost. Currently, polyhedral elements are less widespread in the academia and industry because of their topology and the number surrounding polygons, and a complex algorithm is required to implement polyhedral techniques. Thus, most CFD packages avoid polyhedral mesh generation algorithm. To evaluate the performance, numerical properties and flexibility of polyhedral elements for meshing, additional details are still required. Studies on polyhedral elements are scarce, and further evaluation is required in various areas.

### ACKNOWLEDGMENTS

The study was supported by postgraduate studentship award from the City University of Hong Kong.

### REFERENCES

A. MOCHIDA, Y. TOMINAGA, S. MURAKAMI, R. YOSHIE, T. ISHIHARA and R. OOKA, "Comparison of various  $k-\epsilon$  models and DSM applied to flow around a high-rise building", Report on AIJ cooperative project for CFD. *Wind and Structure*, vol. 5, no. 4-7 (2002), pp. 227–2446.

BERG, M. DE, CHEONG, O., KREVELD, M. VAN, and M. O. MARK, "Computational Geometry Algorithms and Applications", Springer, 2008., 2008.

Blocken B. (2014), "50 years of Computational Wind Engineering: Past, present and future", *Journal of Wind Engineering and Industrial Aerodynamics*, 129, 69–102. doi:10.1016/j.jweia.2014.03.008.

CANONSBURG, T. D. (2012), "ANSYS FLUENT User's Guide", 15317(October).

HEFNY, M. M., and OOKA, R. (2008), “Influence of cell geometry and mesh resolution on large eddy simulation predictions of flow around a single building”, *Building Simulation*, 1(3), 251–260. Doi: 10.1007/s12273-008-8321-7.

M. PERI C , “Simulation of flows in complex geometries: New meshing and solution methods”, *In NAFEMS Seminar: Simulation of Complex Flows (CFD), Application and Trends*, 2004.

RAO V. GARIMELLA, JIBUM KIM, and MARKUS BERNDT, “Polyhedral mesh generation and optimization for non- manifold domains”, Josep Sarrate and Matthew Staten, editors, *Proceedings of the 22nd International Meshing Roundtable*, pages 313-330, Springer Internat. (2014).

YAKHOT, V., ORSZAG, S. A., THANGAM, S., GATSKI, T. B., and SPEZIALE, C. G. (1992). “Development of turbulence models for shear flows by a double expansion technique”, *Physics of Fluids A: Fluid Dynamics*, 4(7), 1510. doi:10.1063/1.858424